




RESEARCH ARTICLE

Open Access



Single-cell analysis of menstrual endometrial tissues defines phenotypes associated with endometriosis

Andrew J. Shih¹ , Robert P. Adelson¹, Himanshu Vashistha¹, Houman Khalili¹, Ashima Nayyar¹, Radha Puran¹, Rixsi Herrera¹, Prodyot K. Chatterjee¹, Annette T. Lee^{1,2}, Alexander M. Truskinovsky^{2,3}, Kristine Elmaliki¹, Margaret DeFranco¹, Christine N. Metz^{1,2*}  and Peter K. Gregersen^{1,2*} 

Abstract

Background: Endometriosis is a common, complex disorder which is underrecognized and subject to prolonged delays in diagnosis. It is accompanied by significant changes in the eutopic endometrial lining.

Methods: We have undertaken the first single-cell RNA-sequencing (scRNA-Seq) comparison of endometrial tissues in freshly collected menstrual effluent (ME) from 33 subjects, including confirmed endometriosis patients (cases) and controls as well as symptomatic subjects (who have chronic symptoms suggestive of endometriosis but have not been diagnosed).

Results: We identify a unique subcluster of proliferating uterine natural killer (uNK) cells in ME-tissues from controls that is almost absent from endometriosis cases, along with a striking reduction of total uNK cells in the ME of cases ($p < 10^{-16}$). In addition, an IGFBP1+ decidualized subset of endometrial stromal cells are abundant in the shed endometrium of controls when compared to cases ($p < 10^{-16}$) confirming findings of compromised decidualization of cultured stromal cells from cases. By contrast, endometrial stromal cells from cases are enriched in cells expressing pro-inflammatory and senescent phenotypes. An enrichment of B cells in the cases ($p = 5.8 \times 10^{-6}$) raises the possibility that some may have chronic endometritis, a disorder which predisposes to endometriosis.

Conclusions: We propose that characterization of endometrial tissues in ME will provide an effective screening tool for identifying endometriosis in patients with chronic symptoms suggestive of this disorder. This constitutes a major advance, since delayed diagnosis for many years is a major clinical problem in the evaluation of these patients. Comprehensive analysis of ME is expected to lead to new diagnostic and therapeutic approaches to endometriosis and other associated reproductive disorders such as female infertility.

Keywords: Menstrual blood, Menstrual effluent, Inflammation, Senescence, Fibrosis, Biomarkers, Decidualization, Endometriosis, Single-cell RNA sequencing

Background

Endometriosis is a common and heterogeneous disorder that is characterized by the growth of endometrial-like tissues outside of the uterus, most commonly in the peritoneal cavity and associated with inflammation [1]. While the pathogenesis of endometriosis is not understood, retrograde menstruation of endometrial cells and

*Correspondence: cmetz@northwell.edu; pgregers@northwell.edu

² Donald and Barbara Zucker School of Medicine, 500 Hofstra Blvd, Hempstead, NY, USA

Full list of author information is available at the end of the article



tissues via the fallopian tubes is one accepted theory for the development of endometriosis lesions in the peritoneal cavity [2, 3]. However, retrograde menstruation occurs in nearly all women [4], yet endometriosis occurs in approximately one in ten females in their reproductive years [3]. Thus, other factors must contribute to the development of endometriosis. While there is a significant genetic component to endometriosis [5], very little is known about how these putative risk alleles function. On the other hand, the eutopic endometrium of patients with endometriosis is significantly different when compared to the endometrium of those without endometriosis, with inflammatory changes noted in the setting of endometriosis [6–9]. We have undertaken a detailed analysis of endometrial tissues and cells present in menstrual effluent (ME), since ME is the critical biological sample transferred to the pelvic cavity, where most endometriosis lesions grow.

Most previous investigations of ME have involved the phenotypic analysis by immunofluorescence, flow cytometry, and/or in vitro culture of single-cell suspensions collected using menstrual cups [10–14]. Our previous flow cytometry studies showed that uterine natural killer (uNK) cells were relatively depleted in ME from endometriosis cases vs. controls [11]. However, this study was limited by the analysis of relatively few cell types in ME, with no assessment of specific subsets of cells. In addition, we demonstrated a defect in decidualization capacity of endometrial stromal cells grown from the ME of patients with endometriosis when compared to ME-stromal cells grown from healthy controls [11, 15]. While these earlier results potentially provided a basis for a screening test for endometriosis, these analyses relied on laborious and expensive cell culture and in vitro assays, making them impractical for clinical application.

Herein, we investigated fresh ME as an unexplored and important biological specimen for the development of non-invasive diagnostics based on the direct analysis of endometrial tissue fragments. We show that ME contains large numbers of shed fragments from endometrial tissues. Using enzymatic digestion of ME and associated tissues followed by single-cell RNA sequencing (scRNA-Seq) analysis, we compared the major cellular differences and gene expression profiles found in ME collected from healthy controls (without symptoms of endometriosis) and patients diagnosed with endometriosis (confirmed by laparoscopic surgery with positive confirmation by pathology), as well as patients with symptoms of endometriosis (e.g., recurrent dysmenorrhea, persistent abdominal bloating, dyspareunia, dysuria, and/or dyschezia) who are not yet diagnosed. In order to gain insight into the pathogenesis of endometriosis, we particularly focused on the phenotypes of stromal and uNK cells in

ME through scRNA-Seq because these are abundant and have been previously shown to be abnormal in patients.

Methods

Human subjects and menstrual effluent collections

Menstrual effluent (ME) was collected as previously described [11, 15]. Briefly, women of reproductive age ($N=33$, age 20–45 years, average age 33.6 years) living in North America who were not pregnant or breastfeeding, who were menstruating, and who were willing to provide ME samples were recruited mainly via social media and consented to the ROSE study (IRB#13-376A; <https://feinstein.northwell.edu/institutes-researchers/institute-molecular-medicine/robert-s-boas-center-for-genomics-and-human-genetics/rose-research-outsmarts-endometriosis>). Women with histologically confirmed endometriosis (determined following excision laparoscopic surgery and documented in a pathology report without revised American Society for Reproductive Medicine (rASRM) staging/classification) were enrolled as “endometriosis” subjects ($N=11$). Women who reported chronic symptoms consistent with endometriosis (e.g., recurrent dysmenorrhea, persistent abdominal bloating, dyspareunia, dysuria, and/or dyschezia), but not yet diagnosed with endometriosis (or not) were enrolled as ‘symptomatic’ subjects ($N=13$). Control subjects living in North America who self-reported no gynecologic history suggestive of a diagnosis of endometriosis (and the absence of polycystic ovarian syndrome, and pelvic inflammatory disease) were recruited mainly via social media and enrolled as “controls” ($N=9$).

Endometriosis, symptomatic, and control subjects collected their ME using an “at home” ME collection kit for 4–8 h on the day of their heaviest menstrual flow (typically day 1 or 2 of the cycle) with a menstrual cup (provided by DIVA International), except for one subject who collected ME using a novel menstrual collection sponge (as previously described [15]). After collection, ME was shipped priority overnight at 4°C to the laboratory for processing. ME collected from menstrual cups was mixed 1:1 with DMEM for processing. For the saturated menstrual collection sponge, ME tissue was collected after rinsing the sponges with PBS to collect cells and tissue. Demographic and gynecologic/health data (including hormone usage, menstrual cycle information, and pain/pain medications) for controls, endometriosis subjects, and symptomatic subjects (and the total cohort) are shown in Table 1.

Immunostaining of ME-derived tissue fragments

ME-derived tissue fragments were obtained from controls, symptomatic subjects, and endometriosis patients ($n=2$ each); tissue fragments were collected by pouring

Table 1 Subject group characteristics—control (CTRL), diagnosed (Dx), and symptomatic (Sx)

	CTRL	Dx	Sx	Total	P value (CTRL vs Dx)
Age (years) (mean ± SD)	33.4 ± 5.4	35.2 ± 4.4	32.3 ± 8.2	33.6 ± 6.3	0.42
BMI (kg/m²) (mean ± SD)	24.2 ± 7.1	28.4 ± 5.4	26.8 ± 7.6	26.5 ± 6.8	0.15
Age at menarche (years) (mean ± SD)	12.0 ± 0.9	11.6 ± 1.6	12.6 ± 1.7	12.0 ± 1.5	0.51
Race/ethnicity					0.34
Caucasian	7/9 (78%)	0/11 (91%)	13/13 (100%)	30/33 (91%)	
Black	1/9 (11%)	0/11 (0%)	0/13 (0%)	1/33 (3%)	
Mixed	1/9 (11%)	0/11 (0%)	0/13 (0%)	1/33 (3%)	
Other	0/9 (0%)	1/11 (9%)	0/13 (0%)	1/33 (3%)	
Hispanic		0/9 (0%)	0/11 (0%)	1/13 (8%)	
Typical cycle length (days)					0.52
21–25 days	0/9 (0%)	1/11 (9%)	3/13 (23%)	4/33 (12%)	
26–31 days	8/9 (89%)	7/11 (64%)	8/13 (62%)	23/33 (70%)	
32–39 days	1/9 (11%)	2/11 (18%)	2/13 (15%)	5/33 (15%)	
> 40 days	0/9 (0%)	1/11 (9%)	0/13 (0%)	1/33 (3%)	
Typical bleed time (days)					0.36
< 3 days	0/9 (0%)	2/11 (18%)	0/13 (0%)	2/33 (6%)	
3–5 days	5/9 (56%)	6/11 (55%)	8/13 (62%)	19/33 (58%)	
6–8 days	4/9 (44%)	3/11 (23%)	5/13 (38%)	12/33 (36%)	
Typical flow					0.96
Light	1/9 (11%)	1/11 (9%)	0/13 (0%)	2/33 (6%)	
Moderate	2/9 (22%)	2/11 (18%)	3/13 (23%)	7/33 (21%)	
Moderately heavy	3/9 (33%)	5/11 (45%)	9/13 (69%)	17/33 (52%)	
Heavy	3/9 (33%)	3/11 (23%)	1/13 (8%)	7/33 (21%)	
Hormone use					0.35
Yes	0/9 (0%)	1/11 (9%) ⁺	1/13 (8%)	2/33 (6%)	
Pain in this cycle					0.06
Yes	5/9 (56%)	10/11 (91%)	13/13 (100%)*	28/33 (85%)	
None	4/9 (44%)	1/11 (9%)	0/13 (0%)	5/33 (15%)	
Mild	2/9 (22%)	3/11 (23%)	3/13 (23%)	8/33 (24%)	
Moderate	3/9 (33%)	6/11 (55%)	4/13 (31%)	13/33 (40%)	
Severe	0/9 (0%)	1/11 (9%)	6/13 (46%)	7/33 (21%)	
Pain medication in this cycle (Midol, Advil, Tylenol, Naproxen, Hydromorphone 2 mg/Baclofen/diazepam/Ketamine 8/10/15 mg)					
Yes	1/9 (11%)	6/11 (55%)	10/13 (77%)	17/33 (52%)	

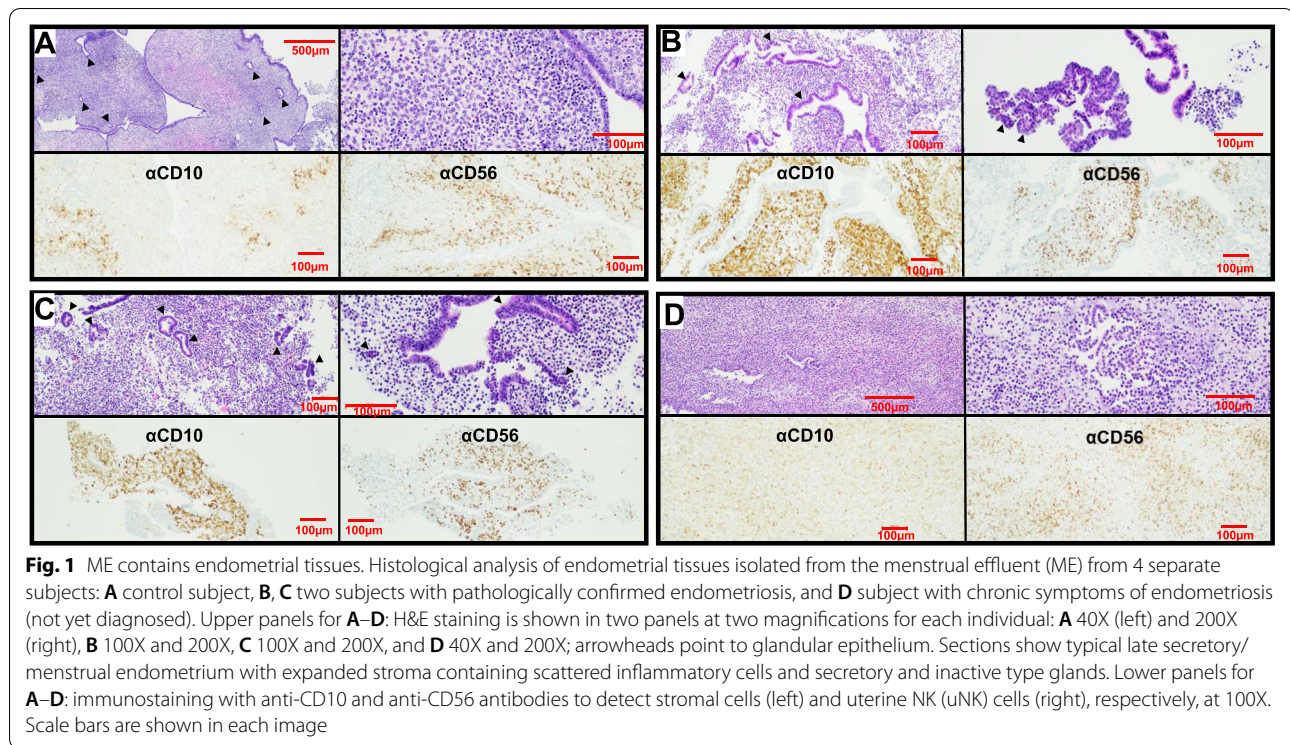
No comparisons of CTRL vs. Sx were significant for the above characteristics, except pain (yes/no): * $p = 0.008$; ⁺one patient used 200mg of progesterone (Prometrium vaginal suppositories) 2 days prior to menses

ME over a 70 μ filter, fixed, and transferred to the clinical pathology lab for paraffin embedding and hematoxylin and eosin (H&E) staining. CD10 was chosen for immunohistochemical analysis because it is a sensitive marker of eutopic endometrial stroma [16] and because adjunctive use of CD10 immunostaining with H&E staining enhances the histologic detection of endometriosis [17]. CD56 was chosen because uNK cells stain brightly with CD56. H&E slides and immunostained

slides were examined microscopically and imaged by a pathologist. Representative images are shown in Fig. 1.

Processing menstrual effluent for scRNA-Seq analyses

Whole (unfractionated) ME (2.5–10 ml) was digested with Collagenase I (1 mg/ml, Worthington Biochemical Corporation, Lakewood, NJ) and DNase I (0.25mg/ml, Worthington Biochemical Corporation) at 37 °C for 10–30 min using the gentleMACS™ Tissue Octo Dissociator (Miltenyi Biotec, Cambridge, MA) using C tubes



and Program 37CMulti_E_01 (31 min). After digestion, the sample was sieved over a 70 μ filter and washed with DMEM 10% fetal bovine serum (FBS) to neutralize digestion enzymes; the flow through was sieved over a 40 μ filter and washed with DMEM 10%FBS. After collecting the single cells (from the flow through) following centrifugation (350 \times g for 5 min), neutrophils were removed using the EasySepTM HLA Chimerism Whole Blood CD66b Positive Selection Kit (STEMCELL, Cambridge, MA), according to the manufacturer's protocol. The neutrophil pellet was frozen at -80°C and used as a source of subject DNA for genotyping (see below). The resultant cells were depleted of red blood cells using the EasySepTM RBC Depletion Reagent (STEMCELL), according to the manufacturer's protocol, and then washed and subjected to density gradient centrifugation using Ficoll-Paque PLUS (Sigma-Aldrich, St. Louis, MO) to collect mononuclear cells, according to manufacturer's directions. To collect ME-tissue, whole ME (2.5–10 ml) was sieved over a 70 μ filter and washed with DMEM; the ME-tissues trapped on the filter were collected and digested with Collagenase I (1mg/ml, Worthington Biochemical Corporation, Lakewood, NJ) and DNase I (0.25mg/ml, Worthington Biochemical Corporation) at 37°C for 10 min and processed as described above for whole ME, except without a density gradient centrifugation step. The resultant whole ME cells were enumerated, and viability was assessed using ViaStainTM AOPI Staining Solution

and the Nexcelom Cellometer (Lawrence, MA). Preparations with $>80\%$ viability were processed for scRNA-Seq. Cells were immediately fixed in methanol for scRNA-Seq, as described by Chen for peripheral blood mononuclear cells [18]. Briefly, cells were washed and resuspended in a 200 μl Ca^{++} and Mg^{++} -free PBS, followed by drop-wise addition of chilled 100% methanol (800 μl , final 80% w/v). Fixed cells were stored at -20°C for 20 min and then stored at -80°C until used for scRNA-Seq. A pilot experiment was performed with a single ME sample, which was processed and either prepared immediately for scRNA-Seq (without methanol fixation and freezing) or was fixed in methanol and frozen, as described above to optimize our scRNA-Seq methods. The data showed almost identical scRNA-Seq results using both methods (see Additional file 1) reassuring us that the methods of Chen et al. [18] can be applied to ME samples. Thus, all ME samples were methanol fixed and frozen. An advantage of this approach is that it allows cost-effective pooling of samples collected at different times and reduces the potential batch effects of running samples separately for scRNA-Seq.

Processing of samples for single-cell sequencing

Methanol-fixed cells were removed from -80°C and placed on ice for 5 min before centrifugation (1000 \times g for 5 min). Methanol-PBS supernatant was completely removed and cells were rehydrated in 0.04% bovine

serum albumin (BSA) + 1 mM dithiothreitol (DTT) + 0.2 U/ μ l RNase Inhibitor in 3X SSC (saline sodium citrate buffer solution) Buffer (Sigma). An aliquot of fixed cells was stained with Trypan Blue and visualized under the microscope. The cells were counted and pooled from different donors at equal ratios, filtered using 40 μ strainer (Falcon), recounted and brought up to a final conc. of 2000 cells/ μ l, and proceeded immediately for GEM generation and barcoding on a 10X Chromium using Next GEM 3' v3.1 reagents (10X Genomics). Libraries were constructed following 10X Genomics' recommendations and quality was assessed on a High Sensitivity DNA chip on a BioAnalyzer 2100 (Agilent) before loading (1.8 pM) and sequencing on an Illumina Nextseq 500 using a High Output kit v2.5 (150 cycles).

Five subjects were pooled together into a single 10X lane with at least one of each phenotype per run with a total of 8 runs for ME-tissue and 3 runs of whole ME. The ME-tissue runs had 44,135 total cells, of which 5147 had ambiguous calls in Demuxlet, 2632 were doublets, and 36,356 were singlets; only the singlets were analyzed. The whole-ME runs had 30,090 total cells, of which 5556 had ambiguous calls, 2776 were doublets, and 21,758 singlets (and hence analyzed). A total of 43,054 cells were analyzed in this study following filtering and QC (thresholds of > 10% mitochondrial reads < 500 nUMI (number of unique molecular identifiers) or > 50000 nUMI or > 6000 unique features per cell).

Single-cell RNA sequencing and analyses and statistics

Samples were converted from raw bcl files to gene by cell matrices using Cell Ranger 6.0 aligned to 10x Genomics' GRCh38-3.0.0 reference. Individuals were demultiplexed via Demuxlet [19] using genotypes taken from SNPs on the Illumina GSAv3 genotyping array, run on DNA prepared from neutrophils isolated from ME. The thresholds in Demuxlet were adjusted to the expected doublet rate, and those marked as doublets were removed. Downstream analysis and visualization were done using Seurat 4.0 [20]. Briefly, there were at least 25,000 reads per cell on average per 10X run, and the mean number of genes captured was 1388 (\pm 896) (mean \pm standard deviation [SD]). There was no significant difference between the various clinical groups (controls, cases, symptomatics) in these values. Genes were filtered out if they were expressed in less than 3 cells while cells were filtered out if they had > 10% mitochondrial reads, 500 < nUMI < 50000 and > 6000 unique features. For the analysis of ME-tissue samples, only subjects with information on at least 500 cells per subject were retained. After filtering, the cell yields were comparable in each group (mean \pm SD: 1256 \pm 732 and 1319 \pm 767 in ME-tissue and whole ME, respectively). Gene expression normalization and

cell clustering was done using the SCTransform pipeline [21] with percent mitochondrial reads regressed out and person specific batch effects corrected using Harmony [22]. Identification of cell clusters was done using known marker genes (Additional file 2) [23–30] with differential gene expression calculated using a Wilcoxon rank sum test. Enrichment of cell clusters of specific phenotypes was done using MASC (mixed-effects modeling of associations of single cells) (<https://github.com/immunogenomics/masc>), which essentially uses a percentage of cells per cluster while also taking into account technical covariates; 10X library batch, preparation (whole ME or ME-tissue), nUMI per cell, percent mitochondrial reads, and phase are accounted for. All datasets are deposited in the National Center for Biotechnology Information/ Gene Expression Omnibus (GEO) accession number GSE203191.

Results

Endometrial tissue fragments are present in fresh menstrual effluent

We carried out histological assessment of fresh menstrual effluent (ME)-associated tissues isolated from ME. Representative H&E sections of ME-derived tissue fragments from four subjects (1 control, 2 laparoscopically/histologically confirmed endometriosis subjects, and 1 symptomatic subject) show the presence of endometrial tissues with mucosal and glandular epithelium and areas of stroma. The endometrium had typical late secretory/ menstrual morphology with expanded stroma containing scattered inflammatory cells and secretory and inactive-type glands (Fig. 1A–D, upper panels). Immunostaining of ME-derived tissue sections reveals a range of stromal cells stained with antibodies to CD10, a clinically used marker of endometrial stroma [16, 17], and an abundance of uNK cells (stained with antibodies to CD56 (NCAM), an archetypical marker of NK cells [Fig. 1A–D, lower panels]).

Single-cell RNA sequencing (scRNA-Seq) of digested freshly processed ME reveals the presence of a heterogeneous mixture of immune and non-immune cells

We have analyzed ME samples from 33 subjects, including age-matched healthy controls ($N=9$), endometriosis cases ($N=11$), and subjects with chronic symptoms suggestive of endometriosis but not yet diagnosed ($N=13$) (see Table 1). ME samples from either whole ME (unfractionated) or ME samples enriched for tissues ("ME-tissue") were digested with collagenase I and DNase I, depleted of neutrophils, and processed for scRNA-Seq, as described in the methods. As shown in Fig. 2, a graph-based clustering approach using Seurat

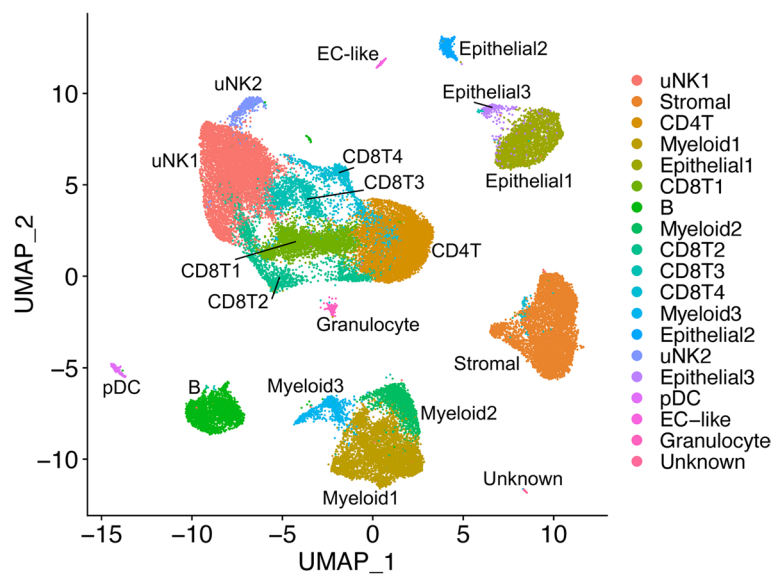


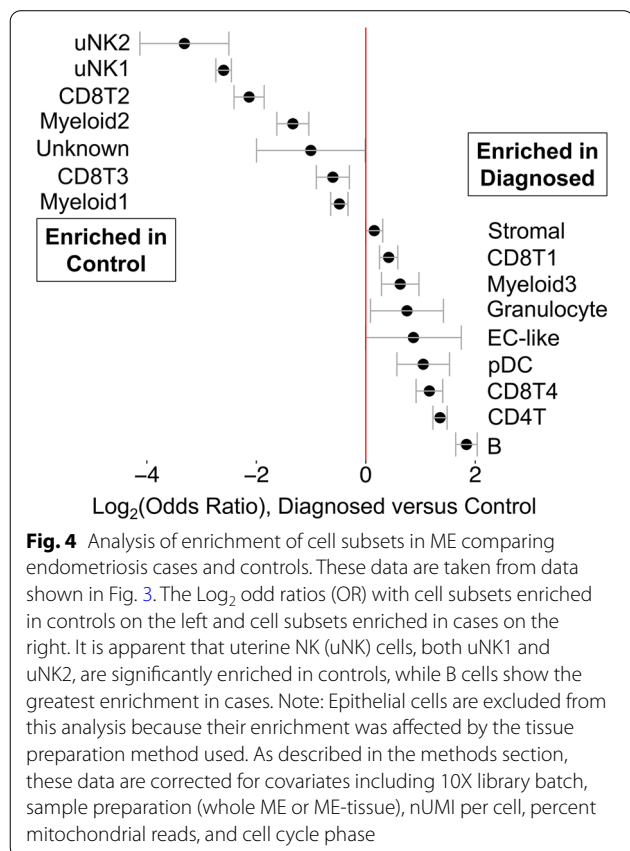
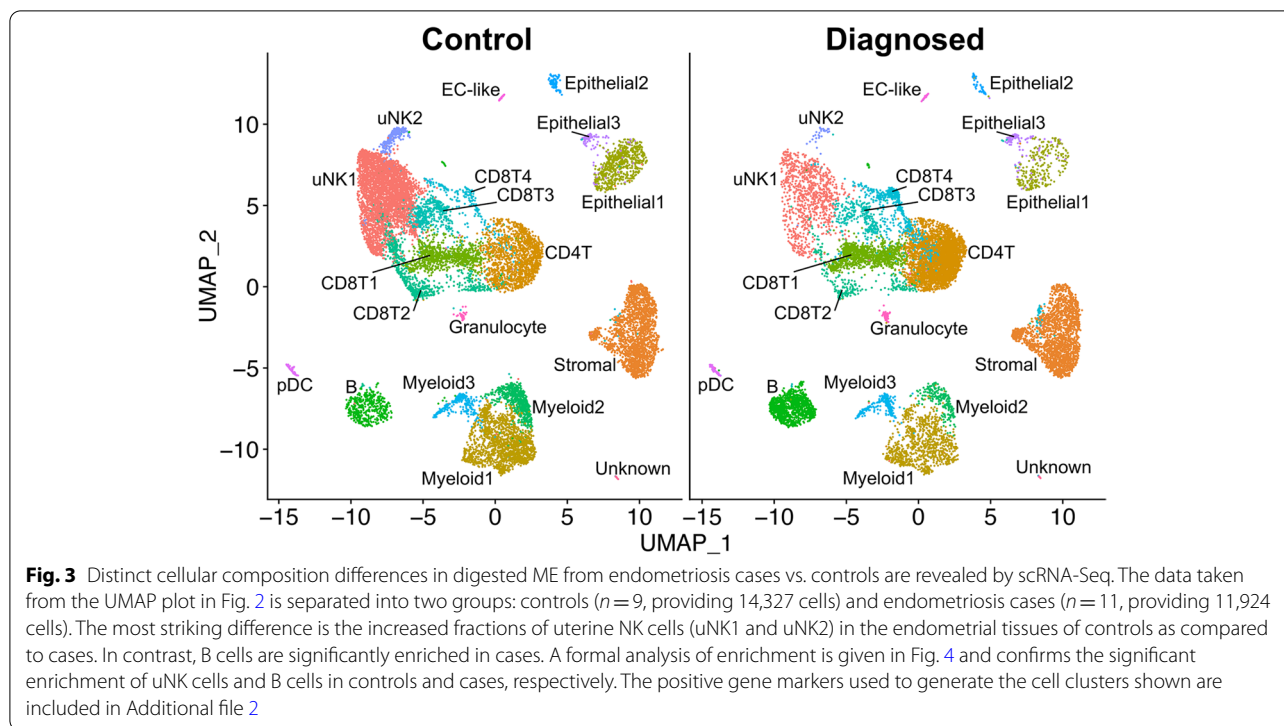
Fig. 2 Cellular composition of digested ME based on scRNA-Seq. UMAP plot for all 33 digested menstrual effluent (ME) samples (controls = 9; endometriosis cases = 11; symptomatic cases = 13). Several well-delineated cell clusters include a large cluster of uterine NK cells (uNK1), as well as clearly separated stromal cells, epithelial cells, and B cells. Several clusters each of T cells and myeloid cells are also defined, as well as a small cluster of plasmacytoid dendritic cells (pDC). A small cluster of approximately 60 unknown cells is in the lower right corner. The positive gene markers used to generate the cell clusters shown are included in Additional file 2.

distinguishes multiple cell clusters shown on the UMAP (uniform manifold approximation and projection) plot. There is striking diversity of the cell types defined by the cluster analysis. A major group of uterine NK cells is designated cluster uNK1, with a small associated cluster designated uNK2. Sets of clusters related to CD8+ and CD4+ T cells are shown in the central portion of the plot. Endometrial stromal cells and epithelial cells are identified in major clusters in the right side of the UMAP plot. Subclusters of endometrial stromal cells are described below in detail. Based on [31], Epithelial1 appears to be a mix of luminal and glandular epithelial cells, Epithelial2 is comprised of ciliated epithelial cells, and Epithelial3 is a separate set of CD326-expressing cells that do not overlap with Epithelial1 or Epithelial2. Distinct clusters of B cells and myeloid cells can also be delineated, along with a small cluster of plasmacytoid dendritic cells (pDC). The positive gene markers used to generate the cell clusters shown in Fig. 2 are included in Additional file 2. Overall, the various cell clusters are well represented whether unfractionated whole ME or tissue-enriched ME is processed for scRNA-Seq. Some differences in cell subset frequencies can be observed; in particular, epithelial cells

were enhanced when tissue-enriched ME was utilized for sample processing (see Additional file 3).

Cell clusters from ME containing endometrial tissue differ between endometriosis cases and healthy controls; relative depletion of uterine NK cells and enrichment of B cells in endometriosis cases

We compared the relative frequency of the various cell clusters in the freshly processed ME obtained from the diagnosed endometriosis cases ($N=11$) compared with controls ($N=9$), as shown in Fig. 3. By inspection of Fig. 3, it is apparent that both clusters of uNK cells (uNK1 and uNK2) are markedly depleted in the cases vs. controls (average percentage of uNK approximately 8% in cases, 28% in controls), as well as an increase in the proportion of B cells in cases (~9%) vs. controls (~3%). The odds ratios and confidence intervals for these two cell enrichment patterns are shown in Fig. 4, along with the patterns of enrichment of all the other major cell clusters. While there is some variation among many of the different cell clusters, a formal analysis shows the most striking differences are observed for uNK cells, which are enriched in controls (and depleted in cases; uNK1, $P < 10E-16$; uNK2, $P < 10E-16$), along



with a relative enrichment in the proportion of B cells in the cases diagnosed with endometriosis (and relatively depleted in controls; $P < 10E-16$). Note that the stromal cell cluster is not significantly different between cases and controls ($P > 0.05$).

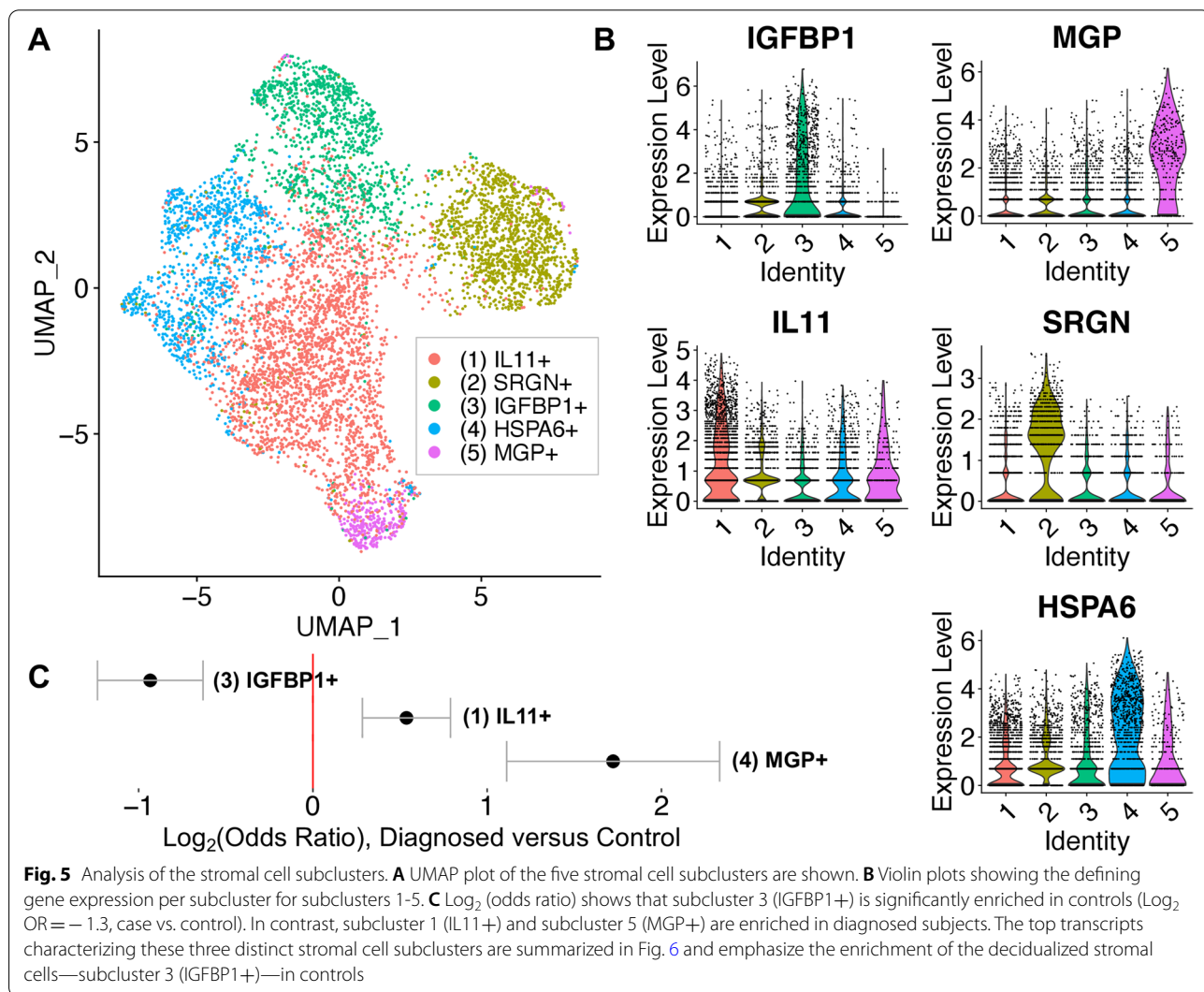
We also explored whether the various proportions of cell clusters of the ME preparations from the “symptomatic” but undiagnosed group of subjects ($N = 13$) are different from ME preparations from controls. This is clearly the case, as shown in Additional file 4. Here, we show the relative enrichment of uNK cells is maintained in controls in comparison to the symptomatic group (uNK1, $P < 10E-16$; uNK2, $P = 0.0025$), similar to that observed with ME from cases. B cells also show a significant relative enrichment in symptomatic as well as diagnosed cases, compared with controls (symptomatic vs. control, $P = 5.8 \times 10^{-6}$), similar to that observed with ME from cases (Additional file 4). Perhaps not surprisingly, these significant differences in symptomatic cases vs. controls are less striking than the differences in endometriosis cases vs. controls, given the likely heterogeneity of the symptomatic group.

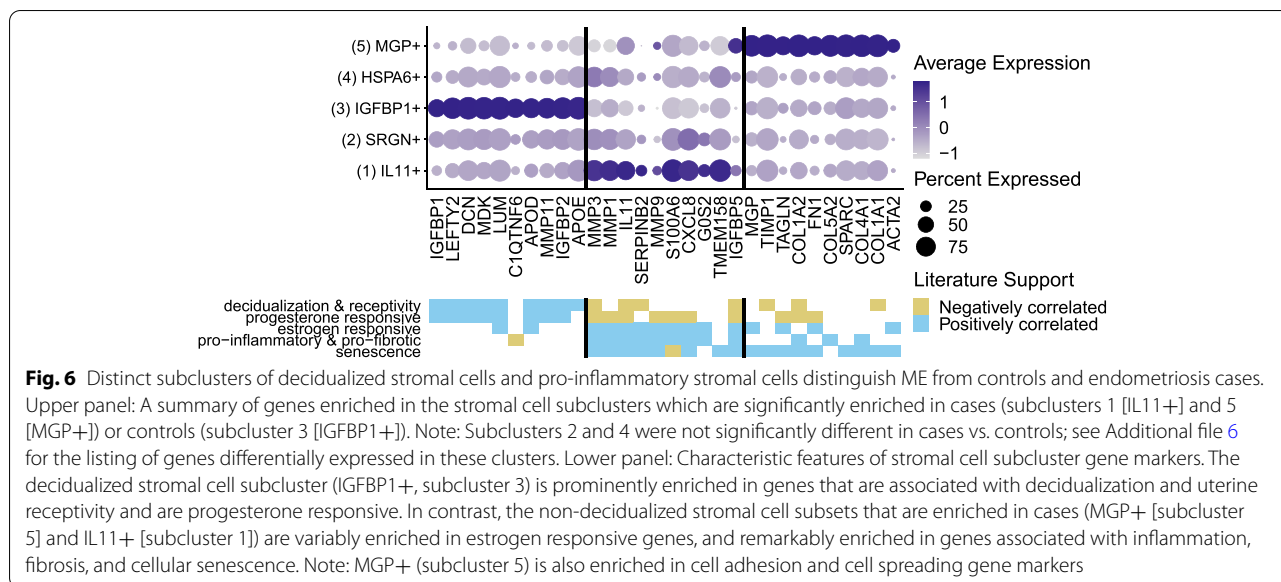
Decidualized stromal cell subclusters are reduced in endometriosis

Previous studies have reported reduced decidualization capacity in endometrial stromal cells grown from biopsies of patients with endometriosis [32]. We have also

observed impaired decidualization using stromal cells grown directly from ME [11, 15]. Therefore, we examined whether this trend could be observed in fresh stromal cells analyzed by scRNA-Seq. The stromal cell numbers or percentages did not significantly differ between the control and endometriosis groups, as shown in Figs. 3 and 4. However, subclustering of the stromal cell cluster clearly identified 5 subclusters of interest within the stromal cell population (Fig. 5A). We have designated these subclusters based on the dominant transcripts expressed in each of these subclusters, as shown in the violin plots in Fig. 5B. Two of the five subclusters (2 and 4) are not different between cases and controls (the top genes of subclusters 2 and 4 are described in Additional file 5). The subclusters showing significant enrichment in either cases or controls (subclusters 1, 3, and 5) are indicated by the Log_2 (odds ratios, [OR]) below the UMAP plot (Fig. 5C).

It is striking that an apparently decidualized stromal cell subcluster (expressing *IGFBP1* mRNA) is significantly enriched in controls compared with endometriosis cases (Fig. 5A, B). In addition to *IGFBP1*, the top differentially expressed genes in this subcluster (compared to other stromal cell subclusters) include *LEFTY2*, *DCN*, *LUM*, *MDK*, *C1QTNF6*, *APOE/D*, *DCN*, and other progesterone sensitive and decidualization/fertility gene markers (see left panel (subcluster 3) in Fig. 6 and Additional file 6 [33–112]). This suggests that a phenotype of “decidualization” can be measured directly in stromal cells derived from fresh ME and is associated with control vs. disease phenotype. A modest enrichment of a subcluster expressing *IL11* was observed in cases, as indicated in Fig. 5A–C. In addition to *IL11*, this subcluster is associated with transcripts for *MMP3*, *MMP1*, *MMP9*, *SERPINB2*, *S100A6*, and *CXCL8*, among other genes associated with inflammation, fibrosis, and senescence,





as well as endometriosis, as shown in the middle panel (subcluster 1) of Fig. 6 (and Additional file 6). A third subcluster, designated by high expression of the gene encoding matrix Gla protein (*MGP*), is also enriched in the stromal cells of cases (Fig. 5A–C). This subset expresses numerous extracellular matrix genes that have been associated with presence of perivascular stromal cells, senescence, and cell adhesion/cell spreading, including *FNI* (which encodes fibronectin-1), a known risk locus for endometriosis [113]. Figure 6 (right panel (subcluster 5) and Additional file 6) also shows the list of top genes expressed in this subset. Additional file 7 demonstrates that the *IGFBP1+* and *MGP+* subclusters map to stromal cells subsets defined in the decidua found in the first trimester of pregnancy by Vento-Tormo et al. [26].

We also examined the differences between cases and controls in the two uNK subclusters present in digested endometrial tissues in ME (uNK1 and uNK2, see Fig. 2). We noted a distinct subcluster of uNK cells (uNK2) that is characterized by the expression of genes associated with cell proliferation such as *MKI67* which encodes Ki67 and *TOP2A* which encodes topoisomerase 2A (see Additional file 8 for a full uNK subcluster analysis). As discussed below, this cluster also mapped nearly exactly (97%) with a proliferative subset of uNK cells that has been defined by scRNA-Seq in decidua obtained during the first trimester of pregnancy [26]. This is consistent with the proliferation of uNK cells and overall accumulation of uNK cells in the course of decidualization in control subjects vs. cases, as shown in Figs. 3 and 4.

Finally, in order to address the possibility that the use of hormone treatment by one endometriosis subject (see

Table 1) might have affected our results, we performed a reanalysis of cases and controls after eliminating this subject. The results are not significantly changed.

Specifically, the overall spatial distribution of the UMAP is not different when the cells from the endometriosis subject on hormones were removed from the data (Additional file 9), and the log₂ odd ratios (OR) for the cell subsets enriched in controls and cell subsets enriched in cases are not different (Additional file 10). Additionally, the clustering of the endometrial stromal cells is not different (Additional file 11) from the original set (with all cases). Comparing all differentially expressed genes with/without the hormone sample in stromal cell subsets and correlating log fold changes of significant genes within each subcluster shows they are highly correlated, $R \geq 0.997$ for all samples (data not shown).

Discussion

These studies show for the first time that the phenotype of eutopic endometrial tissue shed into the menstrual effluent is distinct in patients with endometriosis compared to control subjects. There are three major observations. First, the endometrial stromal cells show a relative deficiency of progesterone-sensitive gene markers associated with endometrial stromal cell decidualization in patients with endometriosis (e.g., *IGFBP1*, *LEFTY2*, *LUM*, *DCN*, etc.). This is consistent with previous studies showing impaired decidualization of cultured endometrial stromal cells obtained from endometrial and ectopic endometriosis biopsies [32, 114], as well as from menstrual effluent [11, 15]. Secondly, there is a striking reduction in the proportion of uNK cells in the ME-derived

endometrial tissue of patients with endometriosis compared with controls. This was suggested by our previous studies of free cells present in ME using flow cytometry methods [11], but it is clearly a major distinguishing feature of the eutopic endometrium of endometriosis patients. Thirdly, our data suggest an enrichment of B cells in the eutopic endometrium of patients with endometriosis, a finding that is consistent with the hypothesis that chronic inflammation and/or chronic endometritis is a predisposing factor in the development of endometriosis [115].

A deficiency in the decidualization capacity of stromal cells cultured from biopsies of the eutopic endometrium has been reported previously [32] and is also found in ME-derived stromal cells collected at the time of menstruation [11, 15]. Our scRNA-Seq data clearly shows the reduction of the *IGFBP1*⁺-expressing decidualized stromal cell subcluster in endometriosis cases vs. controls (Fig. 5C). The relationship of this finding to the pathogenesis of endometriosis is not established. One possibility is that this differentiation deficiency leaves behind non-decidualized endometrial stromal cells that exhibit proinflammatory, pro-fibrotic, and/or senescent phenotypes. These “pathogenic” cells may then initiate or promote lesions following retrograde transfer into the peritoneal cavity. The enrichment of an *IL11*⁺-expressing stromal cell subcluster in the endometriosis ME samples that express many estrogen-responsive, pro-inflammatory, pro-fibrotic, and senescence gene markers (shown in Fig. 6 and Additional file 6) provides some support for this possibility, but this needs confirmation in larger datasets. The significant increase in the *MGP*⁺ stromal subcluster in endometriosis (Fig. 5C) is also of potential interest. As shown in Fig. 6 (right panel), the *MGP*⁺ stromal cell subcluster expresses many genes that are associated with the extracellular matrix, including *FNI* (encoding fibronectin-1) which has been associated with an increased risk for endometriosis in GWAS studies [116]. Interestingly, most of the top markers found in the *IL11*⁺ and the *MGP*⁺ subclusters are either associated with senescence or induce senescence (e.g., *IL11* and *SERPINB2*, see Fig. 6 and Additional file 6). Inflammation and senescence are key features of endometriosis and reduced uterine receptivity and infertility [117–119].

Another possibility is that the overall environment of the eutopic endometrium predisposes to reduced stromal cell decidualization, independent of any direct role or effect on stromal cell subsets in the disease. A chronic inflammatory endometrial environment might lead to, or be associated with, other changes that put individuals at risk for endometriosis. For example, the presence of chronic endometritis has been reported to be a significant risk factor for endometriosis [115, 120]; chronic

endometritis is also associated with reduced stromal cell decidualization [121]. Interestingly, the presence of B cells in endometrial tissue, particularly plasma cells, is a requirement for the clinical diagnosis of chronic endometritis [115]. We note the significant increase in B cells in shed endometrium of endometriosis patients (Figs. 3 and 4) and symptomatic subjects (Additional file 4) when compared to controls. This may reflect an inflammatory state, as B cells play an important role in mediating or regulating inflammatory and autoimmune diseases [122]. The numbers of B cells available for detailed analysis have not allowed us to fully understand the phenotype of these cells; this is an area for future study.

We have demonstrated that uNK cells are remarkably depleted in the ME-derived endometrial tissues of patients with endometriosis (Figs. 3 and 4 and Additional file 4). This may reflect compromised decidualization in these subjects. uNK cells are characteristic of decidualizing tissues [123] and are also prominent in the decidua of early pregnancy [26]. To our knowledge, this is the first report of proliferating uNK cells found in ME. Crosstalk between stromal cells and uNK cells is a feature that promotes decidualization and uterine receptivity/placental vascular remodeling [124]. uNK cells do not appear to play a major role in decidualization in uNK deficient *IL15* knockout mice [125]. It remains unclear whether uNK cells or stromal cells are the primary driver of the decidualization impairment in endometriosis. However, uNK cells do play a role in the maintenance of decidual integrity as reported by Ashkar et al. [126]. Brighton and co-workers emphasized the important role of uNK cells in clearing senescent decidual cells in the cycling human endometrium and their clearance is proposed to be important for optimal fertility [9]. A lack of uNK cells in the endometrium may contribute to increased numbers of senescent cells observed in the stromal subclusters among endometriosis subjects and may contribute to endometriosis-associated infertility. However, it is plausible that a lack of decidualizing endometrial stromal cells (with concomitant reduced production of IL-15 and uNK chemo attractants) reduces the infiltration and proliferation of uNK in decidualizing zones. Defective uNK cell function has recently been proposed in the setting of endometriosis with infertility [127]. We did not observe *IL15* expression by ME-stromal cells; this is not surprising as IL-15 expression by stromal cells peaks before the mid-secretory phase. Interestingly, we did observe enhanced expression of *IL2RB* (which encodes a component of the IL-15 receptor) in the uNK cells of controls compared with the endometriosis group. Since uNK cells are reported to play a role in infertility [123, 128], and infertility is a common feature of endometriosis, further analysis of the uNK subset will clearly be of interest.

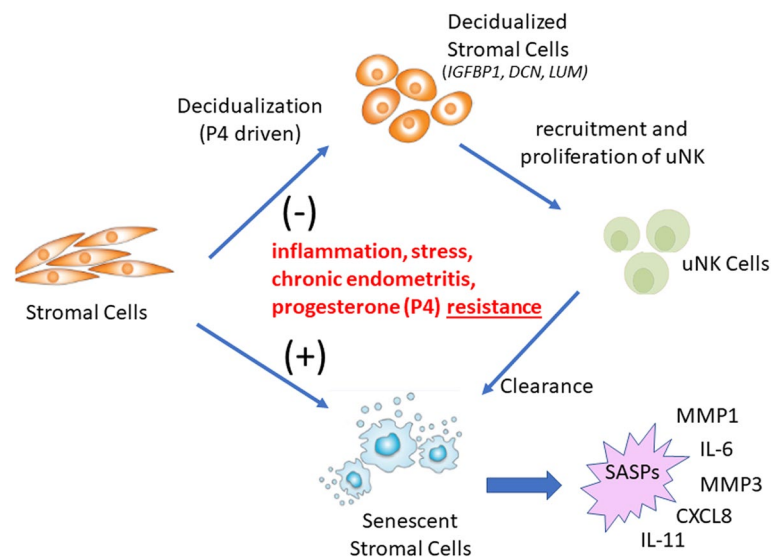


Fig. 7 A disease model for endometriosis. Defective endometrial stromal cell decidualization may be driven by multiple factors including inflammation, chronic endometriitis, stress, and/or progesterone resistance. This, in turn, may direct stromal cell differentiation in the direction of chronic inflammation and senescence, with accompanying senescence-associated secretory phenotypes (SASPs), which include pro-inflammatory mediators and proteases. The senescence phenotype may also impair decidualization. Reduced decidualization may also compromise the infiltration and proliferation of uNK cells, which are likely to be important for senescent cell removal. Further analysis of other cells in menstrual effluent will be important to provide further support for this model

Taken together, these observations suggest a set of interactions that may drive the development and/or progression of endometriosis at several levels, as summarized in Fig. 7. Stromal cell decidualization may be inhibited by a number of factors, including chronic inflammation, stress, and/or progesterone resistance. This may divert stromal cells into a more proinflammatory/senescent state. Furthermore, deficient decidualization may also compromise the infiltration of uNK cells into the decidua and therefore reduce the clearance of senescent cells. Clearly, host genetic variation may influence these processes at every level of these interactions.

It is encouraging that many of our findings in patients with pathologically confirmed endometriosis are also present in a proportion of subjects with chronic symptoms that are suggestive of endometriosis, even in the absence of a confirmed tissue diagnosis. The delay in diagnosis of endometriosis is widely recognized as a major barrier in the management of this disease, with delays of up to a decade in some subjects before the disease is recognized [129]. We recognize the limitation that the symptomatic group lacks a diagnosis, and therefore, we cannot assess the predictive ability of our results. To address this limitation, a clinical trial is underway to enroll symptomatic subjects who are being evaluated by diagnostic laparoscopy as part of their standard care by collaborating surgeons; scRNA-Seq profiles of their ME collected prior to surgery will be validated based on

the results of their laparoscopic diagnosis. Such a study design will be required to establish the positive and negative predictive value of menstrual tissue analysis in a real-world clinical setting where an endometriosis screening test might be applied.

The method of using methanol fixation has been widely used [18], along with other approaches such as cryopreservation, for scRNA-Seq. Despite its advantages, it is possible that methanol fixation may change scRNA-Seq outcomes and relative cell numbers. Therefore, it will be important to replicate these data using a variety of methods. Due to the cost and complexity of the analysis, an scRNA-Seq approach is unlikely to become a diagnostic test for endometriosis. However, we propose that the data obtained from scRNA-Seq can be leveraged to develop future diagnostic and/or screening tests. What should such screening tests involve? It will likely include an assessment of gene expression patterns among ME-derived stromal cells or uNK cells (or specific stromal cell and uNK subsets). An initial analysis of stromal cell clusters suggests several potentially useful gene expression differences among cases vs. controls (Additional file 12). Differences are also observed in uNK cells (Additional file 13) or indeed may be found in other cell types as well. On the other hand, if it can be adapted to a clinical diagnostic test, scRNA-Seq analysis of these tissues is likely to be the most informative approach, perhaps having more global utility to establish complex

and heterogeneous disease subtypes, as well as predicting or following response to therapy. Additional phenotypes that can be uncovered using scRNA-Seq analysis on larger populations may yet yield additional biomarkers that can be incorporated into a more targeted multivariate biomarker analysis for diagnostic purposes.

In any case, the integration of our findings into a unified picture of the pathogenesis of endometriosis will require additional scRNA-Seq studies of larger heterogeneous populations, at different stages of disease development and include deeper analysis of T cells, B cells, myeloid cells, and epithelial cells. Abnormalities of the eutopic endometrium are widely recognized features of endometriosis [6–9], and this can provide diagnostic value, regardless of whether retrograde menstruation plays a causative role. In addition, it is likely that scRNA-Seq approaches of the endometrium via ME may allow for improved classification of clinically meaningful disease subsets and as a means for assessing patients' responses to therapies, as well as uterine-associated fertility status. For example, many of the genes that exhibit changes in the stromal cell subclusters are associated with either estrogen or progesterone responsiveness (Fig. 6), and these differences could be used to guide or assess responses to hormonal therapies and for assessing aspects of uterine receptivity/fertility.

On the other hand, if disease causation is due to retrograde menstruation of abnormal endometrial tissues, ME analysis provides an opportunity to explore new therapies. For example, based on the enrichment of pro-senescent genes in endometriosis endometrial stromal cells (vs. control cells) and the deficit of uNK cells in endometriosis subjects, we propose investigating senescence as a feature of endometriosis. If this can be demonstrated, it may have potential therapeutic implications, since various senotherapeutics (senolytic and senomorphic agents) have now been shown to improve chronic inflammatory diseases in pre-clinical models and human clinical trials [130, 131]. This is significant since none of the current medical therapies for endometriosis have been shown to alter disease progression.

Conclusions

In summary, these scRNA-Seq data of ME collected from endometriosis cases and healthy controls represent a first attempt to globally characterize the cellular diversity of endometrium that is shed at the time of menstruation. More detailed studies in larger datasets are clearly required, particularly regarding diversity in T cells, B cells, and myeloid cells, as well as epithelial cells. We propose that a comprehensive assessment of cellular phenotypes in ME tissues will open a new window on both diagnosis as well as preventive treatment for patients at risk for endometriosis as well as other uterine and reproductive disorders.

Abbreviations

BSA: Bovine serum albumin; DTT: Dithiothreitol; FBS: Fetal bovine serum; GEO: Gene Expression Omnibus; H&E: Hematoxylin and eosin; MASC: Mixed-effects modeling of associations of single cells; ME: Menstrual effluent; nUMI: Number of unique molecular identifiers; OR: Odds ratios; pDC: Plasmacytoid dendritic cells; SASP: Senescence-associated secretory phenotype; scRNA-Seq: Single-cell RNA sequencing; SD: Standard deviation; SSC: Saline sodium citrate; UMAP: Uniform manifold approximation and projection; uNK: Uterine natural killer.

Supplementary Information

The online version contains supplementary material available at <https://doi.org/10.1186/s12916-022-02500-3>.

Additional file 1. Comparison of UMAP plots of ME digests using fresh cells vs. methanol fixation. Virtually identical UMAP plots are observed using either fresh or methanol fixed cells from a single subject. The ME samples were prepared by tissue enrichment and tissue digestion, followed by scRNA-Seq analysis, as described in the methods section.

Additional file 2. Markers for UMAP plots of major cell clusters.

Additional file 3. Cell cluster composition of ME is similar when ME is analyzed after enrichment for endometrial tissues and digested or analyzed as digested whole ME. Comparison of UMAP plots is shown for ME samples prepared by tissue enrichment of menstrual effluent ("ME-Tissue"; 6 diagnosed subjects and 5 controls) or when tissue digestion is applied to unfractionated ME ("whole ME"; 5 diagnosed subjects, and 4 controls). The various cell types are generally well represented between the two approaches to ME preparation. Of note there is an increased yield of epithelial cells in ME samples enriched for tissue. The positive gene markers used to generate the cell clusters shown are included in Additional file 2.

Additional file 4. Cell clusters of ME samples distinguish endometriosis cases and symptomatic cases vs. controls. The combined UMAP plot shown in Fig. 1 is split into controls ($n=9$), cases ($n=11$), and subjects with suggestive symptoms of endometriosis but without laparoscopic tissue diagnosis – the "symptomatic" group ($n=13$). Comparisons of uterine NK (uNK) cell and B cell frequencies in the symptomatic group show a trend that is similar to cases vs. controls. The positive gene markers used to generate the cell clusters shown are included in Additional file 2.

Additional file 5. Top 10 genes in groups 2 and 4 stromal cell subclusters from Figs. 5 and 6.

Additional file 6. References for genes described in Fig. 6.

Additional file 7. Stromal cell subclusters in ME samples map to stromal cell clusters found in first trimester decidua. We have compared the mapping of stromal subclusters reported by Vento-Tormo [26], based on the analysis of decidua in the first trimester, with the mapping of stromal cell subclusters we have described in menstrual effluent (ME). Note that our IGFBP1+ subcluster maps almost identically to the decidualizing stromal cell subset dS2 defined by Vento-Tormo [26]. In addition, our MGP+ subset shows a substantial overlap with dP2 and dP1 of Vento Tormo [26], subsets which are attributed to the perivascular stromal cells in first trimester decidua.

Additional file 8. uNK subclusters reveal a proliferating uNK subcluster enriched in control ME. We have examined subclusters of uterine NK (uNK) cells in our dataset and identified a subcluster whose gene expression patterns reflect cell proliferation, with substantial enrichment of *MKI67* and *TOP2A*. This subset is over 98% matched to a proliferative uNK cell subcluster defined in the decidua of first trimester pregnancy [26]. This subset corresponds to our subset uNK2 that is enriched in controls (Fig. 3).

Additional file 9. The UMAP plot derived from a reanalysis of endometriosis cases ($n=10$) and controls ($n=9$) after removal of one subject on hormones. For this reanalysis, a total of 1112 singlet cells were eliminated from the ME-tissue run from one affected subject on hormones. Only the singlets were analyzed for this revised figure which shows only subtle changes in the details of the UMAP shown in Fig. 3 of the main text.

Additional file 10. A reanalysis of endometriosis cases and controls after removal of one subject on hormones. The Log₂ odd ratios (OR) with cell subsets enriched in controls (n=9) on the left and cell subsets enriched in cases (n=10) on the right. As is the case for Fig. 4 in the main text, it is apparent that uterine NK (uNK) cells, both uNK1 and uNK2, are significantly enriched in controls, while B cells show the greatest enrichment in cases. As noted in the methods section, these data are corrected for covariates including 10X library batch, sample preparation (whole ME or ME-tissue), nUMI per cell, percent mitochondrial reads and phase.

Additional file 11. A reanalysis of stromal cells from endometriosis cases (n=10) and controls (N=9) after removal of one subject on hormones. Not surprisingly, this revised figure shows alterations in the spatial distribution of the UMAP compared to Figure 5 in the main text, but no significant differences in the cell subset distribution comparing cases and controls.

Additional file 12. Stromal cells exhibit distinguishing gene markers differentially regulated in ME from endometriosis cases (n=11) and controls (n=9). Violin plots of the top 10 genes that distinguish endometriosis cases and controls within the total stromal cell population in ME. The data suggest that *IL11* and other transcripts may be useful in distinguishing stromal cells isolated from ME obtained from endometriosis case vs control subjects.

Additional file 13. uNK cells exhibit distinguishing gene markers differentially regulated in ME from endometriosis cases and controls. Violin plots of the top 10 genes that distinguish endometriosis cases (n=11) and controls (n=9) in an analysis of the uNK1 and uNK2 cell subsets as a whole. Note that *IFITM2* and *DNAJA1* expression are substantially higher in ME obtained from endometriosis cases and may provide a useful diagnostic target based on uNK cells that could be purified from tissues isolated from ME.

Acknowledgements

We are grateful to the Endometriosis Foundation of America and to Dr. Tamer Seckin for providing early support for this work and the for the ongoing support from the Northwell Health Innovation Award as well as the constant support provided to PKG by the family of Robert S. Boas. We also thank Anthony Liew, Cassie Pond, and Maruf Chowdhury who provided valuable technical support for this project. We are especially grateful to the many extraordinary patients and volunteers without whose participation this project could not have been accomplished.

Authors' contributions

Conceptualization: CNM, PKG. Recruitment and enrollment: KE, MDF. Data collection: AJS, RPA, KE, HK, MDF. Formal analysis: PKG, CNM, AJS, RPA. Sample processing: RP, PKC, HV, RH, AN. Pathology slide review: AMT. Library construction: HK. Funding acquisition: CNM, PKG. Supervision of scRNA-Seq: ATL. Writing—original draft: PKG, CNM, AJS, RPA. Writing—review and editing: HK, PKG, CNM, RPA, AJS. All authors read and approved the final manuscript.

Funding

This work was supported by the Northwell Health Innovations Award and the Endometriosis Foundation of America.

Availability of data and materials

The original data and materials presented in the study are available from the corresponding authors upon reasonable request. scRNA-Seq data is available at National Center for Biotechnology Information/Gene Expression Omnibus (GEO) (accession number GSE203191).

Declarations

Ethics approval and consent to participate

All procedures for the collection of samples from research subjects were performed with the approval of the institutional review board (IRB) of the Feinstein Institutes/Northwell Health IRB#13-376A. All participants signed informed consent prior to enrollment and study participation.

Consent for publication

All authors give their consent for publication of this manuscript.

Competing interests

The authors declare that they have no competing interests.

Author details

¹Robert S. Boas Center for Genomics and Human Genetics, Feinstein Institutes for Medical Research, Northwell Health, 350 Community Drive, Manhasset, NY 11030, USA. ²Donald and Barbara Zucker School of Medicine, 500 Hofstra Blvd, Hempstead, NY, USA. ³Department of Pathology, North Shore University Hospital, Northwell Health, 300 Community Drive, Manhasset, NY, USA.

Received: 18 February 2022 Accepted: 27 July 2022

Published online: 15 September 2022

References

- International working group of Aagl EE, Wes, Tomassetti C, Johnson NP, Petrozza J, Abrao MS, et al. An International Terminology for Endometriosis, 2021. *J Minim Invasive Gynecol.* 2021;28(11):1849–59.
- Jensen JR, Coddington CC. Evolving spectrum: the pathogenesis of endometriosis. *Clin Obstet Gynecol.* 2010;2:379–88.
- Zondervan KT, Becker CM, Koga K, Missmer SA, Taylor RN, Vignano P. Endometriosis. *Nat Rev Dis Primers.* 2018;4(1):9.
- Halme J, Hammond MG, Hulka JF, Raj SG, Talbert LM. Retrograde menstruation in healthy women and in patients with endometriosis. *Obstet Gynecol.* 1984;64(2):151–4.
- Zondervan KT, Becker CM, Missmer SA. Endometriosis. *N Engl J Med.* 2020;382(13):1244–56.
- Brosens I, Brosens JJ, Benagiano G. The eutopic endometrium in endometriosis: are the changes of clinical significance? *Reprod BioMed Online.* 2012;24(5):496–502.
- Bulun SE. Endometriosis. *N Engl J Med.* 2009;360(3):268–79.
- Vallve-Juanico J, Houshdaran S, Giudice LC. The endometrial immune environment of women with endometriosis. *Hum Reprod Update.* 2019;25(5):564–91.
- Liu H, Lang JH. Is abnormal eutopic endometrium the cause of endometriosis? The role of eutopic endometrium in pathogenesis of endometriosis. *Med Sci Monit.* 2011;17(4):RA92–9.
- van der Molen RG, Schutten JH, van Cranenbroek B, ter Meer M, Donckers J, Scholten RR, et al. Menstrual blood closely resembles the uterine immune micro-environment and is clearly distinct from peripheral blood. *Hum Reprod.* 2014;29(2):303–14.
- Warren LA, Shih A, Renteira SM, Seckin T, Blau B, Simpfendorfer K, et al. Analysis of menstrual effluent: diagnostic potential for endometriosis. *Mol Med.* 2018;24(1):1.
- Schmitz T, Hoffmann V, Olliges E, Bobinger A, Popovici R, Nossner E, et al. Reduced frequency of perforin-positive CD8+ T cells in menstrual effluent of endometriosis patients. *J Reprod Immunol.* 2021;148:103424.
- Hosseini S, Shokri F, Tokhmechy R, Savadi-Shiraz E, Jeddi-Tehrani M, Rahbari M, et al. Menstrual blood contains immune cells with inflammatory and anti-inflammatory properties. *J Obstet Gynaecol Res.* 2015;41(11):1803–12.
- Sabbaj S, Hel Z, Richter HE, Mestecky J, Goepfert PA. Menstrual blood as a potential source of endometrial derived CD3+ T cells. *PLoS One.* 2011;6(12):e28894.
- Nayyar A, Saleem MI, Yilmaz M, DeFranco M, Klein G, Elmalki KM, et al. Menstrual Effluent Provides a Novel Diagnostic Window on the Pathogenesis of Endometriosis. *Front Reprod Health.* 2020;2(3):1–14.
- McCluggage WG, Sumathi VP, Maxwell P. CD10 is a sensitive and diagnostically useful immunohistochemical marker of normal endometrial stroma and of endometrial stromal neoplasms. *Histopathology.* 2001;39(3):273–8.
- Potlog-Nahari C, Feldman AL, Stratton P, Koziol DE, Segars J, Merino MJ, et al. CD10 immunohistochemical staining enhances the histological detection of endometriosis. *Fertil Steril.* 2004;82(1):86–92.
- Chen J, Cheung F, Shi R, Zhou H, Lu W, Consortium CHI. PBMC fixation and processing for Chromium single-cell RNA sequencing. *J Transl Med.* 2018;16(1):198.

19. Kang HM, Subramaniam M, Targ S, Nguyen M, Maliskova L, McCarthy E, et al. Multiplexed droplet single-cell RNA-sequencing using natural genetic variation. *Nat Biotechnol*. 2017;36(1):89–94.
20. Hao Y, Hao S, Andersen-Nissen E, Mauck WM 3rd, Zheng S, Butler A, et al. Integrated analysis of multimodal single-cell data. *Cell*. 2021;184(13):3573–87 e29.
21. Hafemeister C, Satija R. Normalization and variance stabilization of single-cell RNA-seq data using regularized negative binomial regression. *Genome Biol*. 2019;20(1):296.
22. Korsunsky I, Millard N, Fan J, Slowikowski K, Zhang F, Wei K, et al. Fast, sensitive and accurate integration of single-cell data with Harmony. *Nat Methods*. 2019;16(12):1289–96.
23. Wang F, Qualls AE, Marques-Fernandez L, Colucci F. Biology and pathology of the uterine microenvironment and its natural killer cells. *Cell Mol Immunol*. 2021;18(9):2101–13.
24. Queckborner S, von Grothusen C, Boggavarapu NR, Francis RM, Davies LC, Gemzell-Danielsson K. Stromal Heterogeneity in the Human Proliferative Endometrium—A Single-Cell RNA Sequencing Study. *J Pers Med*. 2021;11(6):448.
25. Andreatta M, Corria-Osorio J, Muller S, Cubas R, Coukos G, Carmona SJ. Interpretation of T cell states from single-cell transcriptomics data using reference atlases. *Nat Commun*. 2021;12(1):2965.
26. Vento-Tormo R, Efmova M, Botting RA, Turco MY, Vento-Tormo M, Meyer KB, et al. Single-cell reconstruction of the early maternal-fetal interface in humans. *Nature*. 2018;563(7731):347–53.
27. Dinh HQ, Lin X, Abbasi F, Nameki R, Haro M, Olingy CE, et al. Single-cell transcriptomics identifies gene expression networks driving differentiation and tumorigenesis in the human fallopian tube. *Cell Rep*. 2021;35(2):108978.
28. Lee RD, Munro SA, Knutson TP, LaRue RS, Heltemes-Harris LM, Farrar MA. Single-cell analysis identifies dynamic gene expression networks that govern B cell development and transformation. *Nat Commun*. 2021;12(1):6843.
29. Collin M, McGovern N, Haniffa M. Human dendritic cell subsets. *Immunology*. 2013;140(1):22–30.
30. Chambers SEJ, Pathak V, Pedrini E, Soret L, Gendron N, Guerin CL, et al. Current concepts on endothelial stem cells definition, location, and markers. *Stem Cells Transl Med*. 2021;10(Suppl 2):S54–61.
31. Garcia-Alonso L, Handfield LF, Roberts K, Nikolakopoulou K, Fernando RC, Gardner L, et al. Mapping the temporal and spatial dynamics of the human endometrium in vivo and in vitro. *Nat Genet*. 2021;53(12):1698–711.
32. Barragan F, Irwin JC, Balayan S, Erikson DW, Chen JC, Houshdaran S, et al. Human endometrial fibroblasts derived from mesenchymal progenitors inherit progesterone resistance and acquire an inflammatory phenotype in the endometrial niche in endometriosis. *Biol Reprod*. 2016;94(5):118.
33. Satterfield MC, Hayashi K, Song G, Black SG, Bazer FW, Spencer TE. Progesterone regulates FGF10, MET, IGFBP1, and IGFBP3 in the endometrium of the ovine uterus. *Biol Reprod*. 2008;79(6):1226–36.
34. Young CH, Snow B, DeVore SB, Mohandass A, Nemmara VV, Thompson PR, et al. Progesterone stimulates histone citrullination to increase IGFBP1 expression in uterine cells. *Reproduction*. 2021;162(2):117–27.
35. Ujvari D, Jakson I, Babayeva S, Salamon D, Rethi B, Gidlof S, et al. Dysregulation of in vitro decidualization of human endometrial stromal cells by insulin via transcriptional inhibition of forkhead box protein O1. *PLoS One*. 2017;12(1):e0171004.
36. Fei W, Kijima D, Hashimoto M, Hashimura M, Oguri Y, Kajita S, et al. A functional role of LEFTY during progesterone therapy for endometrial carcinoma. *Cell Commun Signal*. 2017;15(1):56.
37. Takano M, Lu Z, Goto T, Fusi L, Higham J, Francis J, et al. Transcriptional cross talk between the forkhead transcription factor forkhead box O1A and the progesterone receptor coordinates cell cycle regulation and differentiation in human endometrial stromal cells. *Mol Endocrinol*. 2007;21(10):2334–49.
38. Ono YJ, Terai Y, Tanabe A, Hayashi A, Hayashi M, Yamashita Y, et al. Decorin induced by progesterone plays a crucial role in suppressing endometriosis. *J Endocrinol*. 2014;223(2):203–16.
39. Halari CD, Nandi P, Jeyarajah MJ, Renaud SJ, Lala PK. Decorin production by the human decidua: role in decidual cell maturation. *Mol Hum Reprod*. 2020;26(10):784–96.
40. Tamm-Rosenstein K, Simm J, Suhorutshenko M, Salumets A, Metsis M. Changes in the transcriptome of the human endometrial Ishikawa cancer cell line induced by estrogen, progesterone, tamoxifen, and mifepristone (RU486) as detected by RNA-sequencing. *PLoS One*. 2013;8(7):e68907.
41. Salgado RM, FR, Zorn TMT. Modulation of small leucine-rich proteoglycans (SLRPs) expression in the mouse uterus by estradiol and progesterone. *Reprod Biol Endocrinol*. 2011;9(9):22.
42. Lucariello A, TE, Boccia O, Perna A, Sellitto C, Castald MA, et al. Small leucine rich proteoglycans are differently distributed in normal and pathological endometrium. *In Vivo*. 2015;29:217–22.
43. Martin SS, MS-SM, Ferreira S, de Oliveira F, Aplin FJD, Abrahamsohn P, et al. Small leucine-rich proteoglycans (SLRPs) in uterine tissues during pregnancy in mice. *Reproduction*. 2003;125:585–95.
44. Do Carmo S, Seguin D, Milne R, Rassart E. Modulation of apolipoprotein D and apolipoprotein E mRNA expression by growth arrest and identification of key elements in the promoter. *J Biol Chem*. 2002;277(7):5514–23.
45. Kao LC, TS, Lobo S, Imani B, Yang JP, Gemeyer A, et al. Global gene profiling in human endometrium during the window of implantation. *Endocrinology*. 2002;143:2119–38.
46. Altmae S, Koel M, Vosa U, Adler P, Suhorutshenko M, Laisk-Podar T, et al. Meta-signature of human endometrial receptivity: a meta-analysis and validation study of transcriptomic biomarkers. *Sci Rep*. 2017;7(1):10077.
47. Omar M, Laknaur A, Al-Hendy A, Yang Q. Myometrial progesterone hyper-responsiveness associated with increased risk of human uterine fibroids. *BMC Womens Health*. 2019;19(1):92.
48. Rytkonen KT, Erkenbrack EM, Poutanen M, Elo LL, Pavlicev M, Wagner GP. Decidualization of human endometrial stromal fibroblasts is a multiphasic process involving distinct transcriptional programs. *Reprod Sci*. 2019;26(3):323–36.
49. Giudice LC, Milkowski DA, Lamson G, Rosenfeld RG, Irwin JC. Insulin-like growth factor binding proteins in human endometrium: steroid-dependent messenger ribonucleic acid expression and protein synthesis. *J Clin Endocrinol Metab*. 1991;72(4):779–87.
50. Tarantino S, Verhage HG, Fazleabas AT. Regulation of insulin-like growth factor-binding proteins in the baboon (*Papio anubis*) uterus during early pregnancy. *Endocrinology*. 1992;130(4):2354–62.
51. Jasienska G, Ellison PT, Galbarczyk A, Jasienski M, Kalembe-Drozdz M, Kapiszewska M, et al. Apolipoprotein E (ApoE) polymorphism is related to differences in potential fertility in women: a case of antagonistic pleiotropy? *Proc Biol Sci*. 2015;282(1803):20142395.
52. Garcia AJ, Tom C, Guemes M, Polanco B, Mayorga ME, Wend K, et al. ERalpha signaling regulates MMP3 expression to induce FasL cleavage and osteoclast apoptosis. *J Bone Miner Res*. 2013;28(2):283–90.
53. Keller NR, S-RE, Eisenberg E, Osteen KG. Progesterone exposure prevents matrix metalloproteinase-3 (MMP-3) stimulation by interleukin-1a in human endometrial stromal cells. *J Clin Endocrinol Metab*. 2000;85:11–1619.
54. Yamashita CM, Dolgonos L, Zemans RL, Young SK, Robertson J, Briones N, et al. Matrix metalloproteinase 3 is a mediator of pulmonary fibrosis. *Am J Pathol*. 2011;179(4):1733–45.
55. Luddi A, Marrocco C, Governini L, Semplici B, Pavone V, Luisi S, et al. Expression of Matrix Metalloproteinases and Their Inhibitors in Endometrium: High Levels in Endometriotic Lesions. *Int J Mol Sci*. 2020;21(8):2840.
56. Chen C, Li C, Liu W, Guo F, Kou X, Sun S, et al. Estrogen-induced FOS-like 1 regulates matrix metalloproteinase expression and the motility of human endometrial and decidual stromal cells. *J Biol Chem*. 2020;295(8):2248–58.
57. Lockwood CJ, KG, Hausknecht VA, Papp C, Schatz F. Matrix metalloproteinase and matrix metalloproteinase inhibitor expression in endometrial stromal cells during progestin-initiated decidualization and menstruation-related progestin withdrawal. *Endocrinology*. 1998;139:4607–13.
58. Singer CF, Marbaix E, Kokorine I, Lemoine P, Donnez J, Eeckhout Y, et al. Paracrine stimulation of interstitial collagenase (MMP-1) in the human endometrium by interleukin 1alpha and its dual block by ovarian steroids. *Proc Natl Acad Sci U S A*. 1997;94(19):10341–5.

59. Ghosh K, Capell BC. The senescence-associated secretory phenotype: critical effector in skin cancer and aging. *J Invest Dermatol*. 2016;136(11):2133–9.
60. Basisty N, Kale A, Jeon OH, Kuehnemann C, Payne T, Rao C, et al. A proteomic atlas of senescence-associated secretomes for aging biomarker development. *PLoS Biol*. 2020;18(1):e3000599.
61. von Rango U, Alfer J, Kertschanska S, Kemp B, Muller-Newen G, Heinrich PC, et al. Interleukin-11 expression: its significance in eutopic and ectopic human implantation. *Mol Hum Reprod*. 2004;10(11):783–92.
62. Ng B, Cook SA, Schafer S. Interleukin-11 signaling underlies fibrosis, parenchymal dysfunction, and chronic inflammation of the airway. *Exp Mol Med*. 2020;52(12):1871–8.
63. Ng B, Dong J, Viswanathan S, Widjaja AA, Paleja BS, Adami E, et al. Fibroblast-specific IL11 signaling drives chronic inflammation in murine fibrotic lung disease. *FASEB J*. 2020;34(9):11802–15.
64. Chen H, Chen H, Liang J, Gu X, Zhou J, Xie C, et al. TGF-beta1/IL-11/MEK/ERK signaling mediates senescence-associated pulmonary fibrosis in a stress-induced premature senescence model of Bmi-1 deficiency. *Exp Mol Med*. 2020;52(1):130–51.
65. Dimitriadis E, Stoikos C, Stafford-Bell M, Clark I, Paiva P, Kovacs G, et al. Interleukin-11, IL-11 receptor alpha and leukemia inhibitory factor are dysregulated in endometrium of infertile women with endometriosis during the implantation window. *J Reprod Immunol*. 2006;69(1):53–64.
66. Gubbels Bupp MR, Jorgensen TN, Kotzin BL. Identification of candidate genes that influence sex hormone-dependent disease phenotypes in mouse lupus. *Genes Immun*. 2008;9(1):47–56.
67. Schroder WA, Le TT, Major L, Street S, Gardner J, Lambly E, et al. A physiological function of inflammation-associated SerpinB2 is regulation of adaptive immunity. *J Immunol*. 2010;184(5):2663–70.
68. Hsieh HH, Chen YC, Jhan JR, Lin JJ. The serine protease inhibitor serpinB2 binds and stabilizes p21 in senescent cells. *J Cell Sci*. 2017;130(19):3272–81.
69. Park SR, Lee JW, Kim SK, Yu WJ, Lee SJ, Kim D, et al. The impact of fine particulate matter (PM) on various beneficial functions of human endometrial stem cells through its key regulator SERPINB2. *Exp Mol Med*. 2021;53(12):1850–65.
70. Zhang X, Christenson LK, Nothnick WB. Regulation of MMP-9 expression and activity in the mouse uterus by estrogen. *Mol Reprod Dev*. 2007;74(3):321–31.
71. Ahmad N, Chen S, Wang W, Kapila S. 17beta-estradiol Induces MMP-9 and MMP-13 in TMJ Fibrochondrocytes via Estrogen Receptor alpha. *J Dent Res*. 2018;97(9):1023–30.
72. Marbaix EDJ, Courtoy PJ, Eeckhout Y. Progesterone regulates the activity of collagenase and related gelatinases A and B in human endometrial explants. *Proc Natl Acad Sci USA*. 1992;89:11789–93.
73. Steenport M, Khan KM, Du B, Barnhard SE, Dannenberg AJ, Falcone DJ. Matrix metalloproteinase (MMP)-1 and MMP-3 induce macrophage MMP-9: evidence for the role of TNF-alpha and cyclooxygenase-2. *J Immunol*. 2009;183(12):8119–27.
74. Su L, Dong Y, Wang Y, Wang Y, Guan B, Lu Y, et al. Potential role of senescent macrophages in radiation-induced pulmonary fibrosis. *Cell Death Dis*. 2021;12(6):527.
75. Hong EJ, Park SH, Choi KC, Leung PC, Jeung EB. Identification of estrogen-regulated genes by microarray analysis of the uterus of immature rats exposed to endocrine disrupting chemicals. *Reprod Biol Endocrinol*. 2006;4:49.
76. Ghezzi F, Berta GN, Beccaro M, D'Avolio A, Racca S, Conti G, et al. Calcyclin gene expression modulation by medroxyprogesterone acetate. *Biochem Pharmacol*. 1997;54(2):299–305.
77. Xia C, Braunstein Z, Toomey AC, Zhong J, Rao X. S100 proteins as an important regulator of macrophage inflammation. *Front Immunol*. 2017;8:1908.
78. Landi C, Bargagli E, Carleo A, Refini RM, Bennett D, Bianchi L, et al. Bronchoalveolar lavage proteomic analysis in pulmonary fibrosis associated with systemic sclerosis: S100A6 and 14-3-3epsilon as potential biomarkers. *Rheumatology (Oxford)*. 2019;58(1):165–78.
79. Slomnicki LP, Lesniak W. S100A6 (calcyclin) deficiency induces senescence-like changes in cell cycle, morphology and functional characteristics of mouse NIH 3T3 fibroblasts. *J Cell Biochem*. 2010;109(3):576–84.
80. Haim K, Weitzenfeld P, Meshel T, Ben-Baruch A. Epidermal growth factor and estrogen act by independent pathways to additively promote the release of the angiogenic chemokine CXCL8 by breast tumor cells. *Neoplasia*. 2011;13(3):230–43.
81. Armstrong GM, Maybin JA, Murray AA, Nicol M, Walker C, Saunders PTK, et al. Endometrial apoptosis and neutrophil infiltration during menstruation exhibits spatial and temporal dynamics that are recapitulated in a mouse model. *Sci Rep*. 2017;7(1):17416.
82. Russo RC, Garcia CC, Teixeira MM, Amaral FA. The CXCL8/IL-8 chemokine family and its receptors in inflammatory diseases. *Expert Rev Clin Immunol*. 2014;10(5):593–619.
83. Konno R, Y-OH, Fujiwara H, Uchide I, Shibahara H, Okwada M, et al. Role of immunoreactions and mast cells in pathogenesis of human endometriosis -morphologic study and gene expression analysis. *Hum Cell*. 2003;16(3):141–9.
84. Luckow Invitti A, Schor E, Martins Parreira R, Kopelman A, Kamer-gorodsky G, Goncalves GA, et al. Inflammatory cytokine profile of cocultivated primary cells from the endometrium of women with and without endometriosis. *Mol Med Rep*. 2018;18(2):1287–96.
85. Acosta JC, O'Loughlin A, Banito A, Guijarro MV, Augert A, Raguz S, et al. Chemokine signaling via the CXCR2 receptor reinforces senescence. *Cell*. 2008;133(6):1006–18.
86. Carleton JB, Berrett KC, Gertz J. Multiplex enhancer interference reveals collaborative control of gene regulation by estrogen receptor alpha-bound enhancers. *Cell Syst*. 2017;5(4):333–44 e5.
87. Heckmann BL, Zhang X, Xie X, Liu J. The G0/G1 switch gene 2 (G0S2): regulating metabolism and beyond. *Biochim Biophys Acta*. 2013;1831(2):276–81.
88. Barradas M, Gonos ES, Zebede Z, Kolettas E, Petropoulou C, Delgado MD, et al. Identification of a candidate tumor-suppressor gene specifically activated during Ras-induced senescence. *Exp Cell Res*. 2002;273(2):127–37.
89. Hu WP, Tay SK, Zhao Y. Endometriosis-specific genes identified by real-time reverse transcription-polymerase chain reaction expression profiling of endometriosis versus autologous uterine endometrium. *J Clin Endocrinol Metab*. 2006;91(1):228–38.
90. Andrade PM, Silva ID, Borra RC, Lima GR, Baracat EC. Estrogen and selective estrogen receptor modulator regulation of insulin-like growth factor binding protein 5 in the rat uterus. *Gynecol Endocrinol*. 2002;16(4):265–70.
91. Nguyen X-X, Muhammad N, Nietert PJ, Feghali-Bostwick C. IGFBP-5 Promotes Fibrosis via Increasing Its Own Expression and That of Other Pro-fibrotic Mediators. *Front Endocrinol*. 2018;9:eaa7533.
92. Kim KS, Seu YB, Baek SH, Kim MJ, Kim KJ, Kim JH, et al. Induction of cellular senescence by insulin-like growth factor binding protein-5 through a p53-dependent mechanism. *Mol Biol Cell*. 2007;18(11):4543–52.
93. Sanada F, Taniyama Y, Muratsu J, Otsu R, Shimizu H, Rakugi H, et al. IGF binding protein-5 induces cell senescence. *Front Endocrinol (Lausanne)*. 2018;9:53.
94. Salihi DAM, TG, Holding C, Szeszak TAM, Gonzalez MI, Carter EJ, et al. Insulin-like growth factor-binding protein 5 (Igfbp5) compromises survival, growth, muscle development, and fertility in mice. *PNAS*. 2004;101:4314–9.
95. Sheikh MS, Shao ZM, Chen JC, Fontana JA. Differential regulation of matrix Gla protein (MGP) gene expression by retinoic acid and estrogen in human breast carcinoma cells. *Mol Cell Endocrinol*. 1993;92(2):153–60.
96. Dressman MA, Walz TM, LC, Barnes L, Buchholtz S, Kwon I, et al. Genes that co-cluster with estrogen receptor alpha in microarray analysis of breast biopsies. *Pharmacogenomics J*. 2001;1:135–41.
97. Han L, Li X, Zhang G, Xu Z, Gong D, Lu F, et al. Pericardial interstitial cell senescence responsible for pericardial structural remodeling in idiopathic and postsurgical constrictive pericarditis. *J Thorac Cardiovasc Surg*. 2017;154(3):966–75 e4.
98. Kumari R, Jat P. Mechanisms of cellular senescence: cell cycle arrest and senescence associated secretory phenotype. *Front Cell Dev Biol*. 2021;9:645593.
99. Stille JA, Birt JA, Nagel SC, Sutovsky M, Sutovsky P, Sharpe-Timms KL. Neutralizing TIMP1 restores fecundity in a rat model of endometriosis and treating control rats with TIMP1 causes anomalies in ovarian function and embryo development. *Biol Reprod*. 2010;83(2):185–94.
100. Wang J, Jarrett J, Huang CC, Satcher RL Jr, Levenson AS. Identification of estrogen-responsive genes involved in breast cancer metastases to the bone. *Clin Exp Metastasis*. 2007;24(6):411–22.

101. Kunzmann S, Ottensmeier B, Speer CP, Fehrholz M. Effect of progesterone on Smad signaling and TGF-beta/Smad-regulated genes in lung epithelial cells. *PLoS One*. 2018;13(7):e0200661.
102. Thweatt R, Lumpkin CK Jr, Goldstein S. A novel gene encoding a smooth muscle protein is overexpressed in senescent human fibroblasts. *Biochem Biophys Res Commun*. 1992;187(1):1–7.
103. Vafashoar F, Mousavizadeh K, Poormoghimi H, Haghghi A, Pashangzadeh S, Mojtavani N. Progesterone aggravates lung fibrosis in a mouse model of systemic sclerosis. *Front Immunol*. 2021;12:742227.
104. Schafer MJ, White TA, Iijima K, Haak AJ, Ligresti G, Atkinson EJ, et al. Cellular senescence mediates fibrotic pulmonary disease. *Nat Commun*. 2017;8:14532.
105. Kim TH, Yoo JY, Choi KC, Shin JH, Leach RE, Fazleabas AT, et al. Loss of HDAC3 results in nonreceptive endometrium and female infertility. *Sci Transl Med*. 2019;11(474).
106. DeNardo DG, Kim HT, Hilsenbeck S, Cuba V, Tsimelzon A, Brown PH. Global gene expression analysis of estrogen receptor transcription factor cross talk in breast cancer: identification of estrogen-induced/activator protein-1-dependent genes. *Mol Endocrinol*. 2005;19(2):362–78.
107. Cao W, Mah K, Carroll RS, Slayden OD, Brenner RM. Progesterone withdrawal up-regulates fibronectin and integrins during menstruation and repair in the rhesus macaque endometrium. *Hum Reprod*. 2007;22(12):3223–31.
108. Chen G, Liu L, Sun J, Zeng L, Cai H, He Y. Foxf2 and Smad6 co-regulation of collagen 5A2 transcription is involved in the pathogenesis of intrauterine adhesion. *J Cell Mol Med*. 2020;24(5):2802–18.
109. Chan JM, Ho SH, Tai IT. Secreted protein acidic and rich in cysteine-induced cellular senescence in colorectal cancers in response to irinotecan is mediated by P53. *Carcinogenesis*. 2010;31(5):812–9.
110. Urushiyama H, Terasaki Y, Nagasaka S, Terasaki M, Kunugi S, Nagase T, et al. Role of alpha1 and alpha2 chains of type IV collagen in early fibrotic lesions of idiopathic interstitial pneumonias and migration of lung fibroblasts. *Lab Invest*. 2015;95(8):872–85.
111. Lee Y, Shivashankar GV. Analysis of transcriptional modules during human fibroblast ageing. *Sci Rep*. 2020;10(1):19086.
112. Teo YV, Rattanavirotkul N, Olova N, Salzano A, Quintanilla A, Tarrats N, et al. Notch signaling mediates secondary senescence. *Cell Rep*. 2019;27(4):997–1007 e5.
113. Matalliotaki C, Matalliotakis M, Rahmioglu N, Mavromatidis G, Matalliotakis I, Koumantakis G, et al. Role of FN1 and GREB1 gene polymorphisms in endometriosis. *Mol Med Rep*. 2019;20(1):111–6.
114. Klemmt PA, Carver JG, Kennedy SH, Koninckx PR, Mardon HJ. Stromal cells from endometriotic lesions and endometrium from women with endometriosis have reduced decidualization capacity. *Fertil Steril*. 2006;85(3):564–72.
115. Cicinelli E, Trojano G, Mastromauro M, Vimercati A, Marinaccio M, Mitola PC, et al. Higher prevalence of chronic endometritis in women with endometriosis: a possible etiopathogenetic link. *Fertil Steril*. 2017;108(2):289–95 e1.
116. Sapkota Y, Steinhorsdottir V, Morris AP, Fassbender A, Rahmioglu N, De Vivo I, et al. Meta-analysis identifies five novel loci associated with endometriosis highlighting key genes involved in hormone metabolism. *Nat Commun*. 2017;8:15539.
117. Tomari H, Kawamura T, Asanoma K, Egashira K, Kawamura K, Honjo K, et al. Contribution of senescence in human endometrial stromal cells during proliferative phase to embryo receptivity. *Biol Reprod*. 2020;103(1):104–13.
118. Lin X, Dai Y, Tong X, Xu W, Huang Q, Jin X, et al. Excessive oxidative stress in cumulus granulosa cells induced cell senescence contributes to endometriosis-associated infertility. *Redox Biol*. 2020;30:101431.
119. Yu CX, Song JH, Li YF, Tuo Y, Zheng JJ, Miao RJ, et al. Correlation between replicative senescence of endometrial gland epithelial cells in shedding and non-shedding endometria and endometriosis cyst during menstruation. *Gynecol Endocrinol*. 2018;34(11):981–6.
120. Takebayashi A, Kimura F, Kishi Y, Ishida M, Takahashi A, Yamanaka A, et al. The association between endometriosis and chronic endometritis. *PLoS One*. 2014;9(2):e88354.
121. Wu D, Kimura F, Zheng L, Ishida M, Niwa Y, Hirata K, et al. Chronic endometritis modifies decidualization in human endometrial stromal cells. *Reprod Biol Endocrinol*. 2017;15(1):16.
122. Miyagaki T, Fujimoto M, Sato S. Regulatory B cells in human inflammatory and autoimmune diseases: from mouse models to clinical research. *Int Immunol*. 2015;27(10):495–504.
123. Sojka DK, Yang L, Yokoyama WM. Uterine natural killer cells. *Front Immunol*. 2019;10:960.
124. Zhang Y, Wang Y, Wang XH, Zhou WJ, Jin LP, Li MQ. Crosstalk between human endometrial stromal cells and decidual NK cells promotes decidualization in vitro by upregulating IL25. *Mol Med Rep*. 2018;17(2):2869–78.
125. Bany BM, Scott CA, Eckstrum KS. Analysis of uterine gene expression in interleukin-15 knockout mice reveals uterine natural killer cells do not play a major role in decidualization and associated angiogenesis. *Reproduction*. 2012;143(3):359–75.
126. Ashkar AA, Black GP, Wei Q, He H, Liang L, Head JR, et al. Assessment of requirements for IL-15 and IFN regulatory factors in uterine NK cell differentiation and function during pregnancy. *J Immunol*. 2003;171(6):2937–44.
127. Jorgensen H, Fedorcsak P, Isaacson K, Tevonian E, Xiao A, Beste M, et al. Endometrial cytokines in patients with and without endometriosis evaluated for infertility. *Fertil Steril*. 2022;117(3):629–40.
128. Seshadri S, Sunkara SK. Natural killer cells in female infertility and recurrent miscarriage: a systematic review and meta-analysis. *Hum Reprod Update*. 2014;20(3):429–38.
129. As-Sanie S, Black R, Giudice LC, Gray Valbrun T, Gupta J, Jones B, et al. Assessing research gaps and unmet needs in endometriosis. *Am J Obstet Gynecol*. 2019;221(2):86–94.
130. Kirkland JL, Tchkonja T. Senolytic drugs: from discovery to translation. *J Intern Med*. 2020;288(5):518–36.
131. Wissler Gerdes EO, Zhu Y, Tchkonja T, Kirkland JL. Discovery, development, and future application of senolytics: theories and predictions. *FEBS J*. 2020;287(12):2418–27.

Publisher's Note

Springer Nature remains neutral with regard to jurisdictional claims in published maps and institutional affiliations.

Ready to submit your research? Choose BMC and benefit from:

- fast, convenient online submission
- thorough peer review by experienced researchers in your field
- rapid publication on acceptance
- support for research data, including large and complex data types
- gold Open Access which fosters wider collaboration and increased citations
- maximum visibility for your research: over 100M website views per year

At BMC, research is always in progress.

Learn more biomedcentral.com/submissions

